Regenerable, innovative porous silicon-based polymer-derived ceramics for removal of methylene blue and rhodamine B from textile and environmental waters

(Article begins on next page)

Maria Concetta Bruzzoniti, Marta Appendini, Barbara Onida, Michele Castiglioni, Massimo Del Bubba, Lia Vanzetti, Prasanta Jana, Gian Domenico Sorarù, Luca Rivoira

Regenerable, innovative porous silicon-based polymer-derived ceramics for removal of Methylene Blue and Rhodamine B from textile and environmental waters

Maria Concetta Bruzzoniti*[a], Marta Appendini[a], Barbara Onida[b], Michele Castiglioni[a],

Massimo Del Bubba[c], Lia Vanzetti[d], Prasanta Jana[e], Gian Domenico Sorarù[e], Luca Rivoira[a]

[a]*Department of Chemistry, University of Turin, Via P. Giuria 7, 10125 Turin, Italy.*

[b]*Department of Applied Science and Technology, Polytechnic of Torino, Corso Duca degli Abruzzi 24, 10129 Torino, Italy.*

[c]*Department of Chemistry "Ugo Schiff", University of Florence, Via della Lastruccia 3, 50019 Sesto Fiorentino, Italy.*

[d]*Fondazione Bruno Kessler-CMM-MNF, Via Sommarive 18, 38123 Trento, Italy.*

[e]*Department of Industrial Engineering, University of Trento, Via Sommarive 9, 38123 Trento, Italy*

*Corresponding Author:

Maria Concetta Bruzzoniti

Department of Chemistry, University of Turin

Via P. Giuria 7, 10125 Turin, Italy

E-mail: mariaconcetta.bruzzoniti@unito.it

Phone: +39 011 6705277

Fax: +39 011 6707855

Orcid: 0000-0002-9144-9254

Abstract

The presence of residual color in treated textile wastewater above the regulation limits is still a critical issue in many textile districts. Innovative, polymer-derived ceramics of the Si-C-O system, were here synthesized in order to obtain porous nanocomposites materials where a free carbon phase is dispersed into a silicon carbide/silicon oxycarbide network. The sorbents were comprehensively characterized for the removal of two model water soluble dyes (i.e. the cation Methylene Blue and the zwitterion Rhodamine B). Adsorption is very rapid and controlled by intra-particle and/or film diffusion, depending on dye concentration. Among the nanocomposites studied, the SiOC aerogel (total capacity about 45 mg/g^{-1}, is easily regenerated under mild treatment (250 °C, 2h). Adsorption of dyes is not affected by the matrix composition: removals of 150 mg/L Methylene Blue from river water and simulated textile wastewater with high content of metal ions (2-50 mg/L) and chemical oxygen demand (800 mg/L) was higher than 92% and quantitative for a dye concentration of 1 mg/L.

Keywords: dyes; textile wastewater; adsorption; polymer-derived ceramics; regeneration

Introduction

The treatment and reuse of industrial wastewater deriving from the textile sector is an important issue for the quantity of water employed in the process (about 100 m^3 water per ton of fibre treated are necessary) (Goyal et al. 2010) and the quality of wastewater generated. Textile wastewater is characterized by intense color (residual concentration levels are about tens of milligrams per liter (Goyal et al. 2010)), high chemical oxygen demand (COD), as well as high total suspended solids (TSS). Among these characteristics, the residual color present in the effluents of wastewater treatment plants (WWTPs) operating in textile districts still represents a complex and current issue. According to the Ecological and Toxicological Association of Dyes and Organic Pigments Manufacturers (ETAD), dye levels higher than 0.1-1 mg/L may originate visual pollution, depending of a number of

2

factors, such as the mixing degree of the color effluent plume or discharge, the kind of color present and the depth of the receiving water body (Richardson 2008).

Many papers and specific reviews describe color removal from textile wastewater through different treatment techniques, such as coagulation/flocculation, ultrafiltration, biological degradation, adsorption, oxidation and advanced oxidation processes (Gupta 2009; Singh and Arora 2011; Verma et al. 2012). Among them, although ultrafiltration and nanofiltration (Gupta 2009) techniques are effective for the removal of all classes of dyes, dye molecules may cause clogging of the membrane pores, making this approach of limited use due to the high working pressures and short membrane life-time. Significant energy consumption and high cost of membrane are additional drawbacks of these filtration techniques. Chemical treatment of textile wastewater by coagulating/flocculating agents is not suitable for water soluble dyes and, even more important, the process produces large quantity of sludge (Hai et al. 2007). Although oxidation methods with chlorine, Fenton's reagent and ozone proved to be efficient for color removal from waters, their main drawbacks are the possible side-reactions and high costs. In addition, oxidation by using Fenton's reagent generates sludge that has been managed. Among the different advanced oxidation processes, heterogeneous photocatalysis exhibits interesting removal properties, but its efficiency is strongly dependent upon pH conditions. Other intrinsic drawbacks are the limitation of light penetration, the fouling of catalysts and problems concerning the separation of fine catalyst from the treated water (Gupta 2009). Biological treatment represents an economic approach, even if transformation of recalcitrant compounds can be very slow, leading to poor performances of bioreactors (Pereira et al. 2014).

A valid alternative solution to the above-mentioned methods for the removal of dyes from textile wastewater is represented by the adsorption techniques. Activated carbon is maybe the most used adsorbent in water refinement for a large number of organic molecules and has shown practical utility also for the removal of some kind of dyes, like the basic dyes (Al-Degs et al. 2001). Adsorption of dyes onto activated carbon is controlled not only by surface area and porosity of the sorbent, but

also by the functional groups present in the surface which lead to specific interactions with the sorbate. Also mesoporous silica-based materials are receiving considerable attention as possible sorbents for removal of a wide range of contaminants, including dyes (Tian et al. 2016), due to their high surface area, large and uniform pore size, and tunable pore structure. These sorbents can be either used as such (Bruzzoniti et al. 2016), in their precursor form still containing the template (Bruzzoniti et al. 2012), after encapsulation of metal nanoparticles (Fiorilli et al. 2017; Rivoira et al. 2016) or by grafting functional groups selective towards selected pollutants (Bruzzoniti et al. 2009; Caldarola et al. 2014). Polymer-Derived Ceramics (PDCs), are a novel class of multifunctional nanostructured materials (Colombo 2010) and comprises ceramics of the Si-C (silicon carbide), Si-O-C (silicon oxycarbides) and Si-C-N (silicon carbonitrides) systems (Colombo et al. 2010). PDCs have interesting features that make them useful candidates as sorbents for water purification. Indeed, PDCs with SSA up to 600 -700 m^2/g can be easily obtained and their structure displays, at the same time, a variety of different types of chemical bonds (Si-O, Si-N, Si-C, C=C, C=O) and functional groups (OH, NH, COOH) depending on the composition and pyrolysis atmosphere (Nguyen et al. 2015a; Nguyen et al. 2015b; Zera et al. 2014). For these characteristics, PDCs could show high adsorption capabilities towards different molecules (Meng et al. 2015). In spite of these appealing features, PDCs have been rarely tested as adsorbent materials for water purification (Yu et al. 2016). Our group has recently reported the adsorption behavior of macroporous silicon carbide foams made from preceramic polymers toward non-steroidal anti-inflammatory drugs (NSAIDs) and their metabolites (Jana et al. 2016). In another recent work (Bruzzoniti et al. 2018), we have shown that PDCs aerogels (SiC and SiOC types) and foams have different capabilities to retain dyes from waters, namely Methylene Blue (MB) and Rhodamine B (RB), two model basic, widely used for dyeing cotton, wood and silk (El-Ashtoukhy and Fouad 2015) but also in paper dyeing industries. MB is not considered a strong hazardous compound, but it can cause irritation to the gastrointestinal tract with symptoms like nausea, vomiting and diarrhea and can causes irritation to the skin, in case of dermal

4

exposure (Umoren et al. 2013). RB is potentially genotoxic and carcinogenic (Baldev et al. 2013; Melis 2014).

In this work, we study the adsorption behavior of SiOC and SiC aerogels and foams, detailing the mechanisms controlling the kinetics of the sorption process at different dye concentration, thus covering the possible ranges of concentration in which dye can be found in real conditions. Regeneration of the sorbent is shown and detailed discussion on modification of surface characteristics after regeneration is provided. The performance of the synthesized sorbents is tested for real case situations: the kinetics removal performances were determined in case of dyes present in a river water sample and on a simulated textile wastewater.

Materials and methods

Reagents

Methylene blue (MB) and Rhodamine B (RB), HCOONa and HPLC grade CH_3CN used for the eluent preparation were from Sigma-Aldrich (Milan, Italy). Eluent and standard solutions were prepared in high-purity water (18.2 MΩ cm^{-1} resistivity at 25 °C), produced by an Elix-Milli Q Academic system (Millipore, Vimodrone, MI, Italy).

Determination of dyes

Dyes were determined by HPLC and spectrophotometric detection as described in the Supplementary Data.

Adsorbent preparation and characterization

Polymer derived SiC aerogels were prepared crosslinking a liquid allylhydropolycarbosilane (SMP-10, Starfire Systems, Schenectady, USA) with divinyl benzene (DVB, technical-grade, 80%, CAS: 1321-74-0, Sigma-Aldrich, St. Louis, MO, USA) followed by CO_2 supercritical drying and pyrolysis of the pre-ceramic sample in flowing Ar at 900°C. Similarly, SiOC aerogels were obtained

5

from a low viscosity silicon oil, polyhydridomethylsiloxane (Alfa Aesar, PHMS, MW~1900, CAS: 63148-57-2, Alfa Aesar, Ward Hill, MA, USA) and DVB followed by pyrolysis at 900 °C in Ar flow. Details of the synthesis procedure can be found in the literature(Vallachira Warriam Sasikumar et al. 2016). SiC foams were processed following the template method using PU foams impregnated with a preceramic polymer solution and pyrolysis. A SMP-10/cyclohexane solution was used for the impregnation step. Impregnated foams were subsequently dried and pyrolyzed in Ar flow up to 1200°C. Details of the procedure are reported elsewhere (Jana et al. 2017). Details on microstructural characterization of the adsorbents are given in the Supplementary Data section.

Adsorption kinetics and isotherm

Triplicate tests were performed in batch conditions as reported in the Supplementary Data section.

Regeneration and reuse of aerogel

The thermal regeneration was performed on SiOC aerogel after adsorption of 1000 mg/L MB for a contact time of 172 h. The treatment consisted on heating the aerogel in a muffle furnace at 250 °C for 2 h in air. The regeneration conditions were chosen based on the results of a thermogravimetric analysis which showed that the SiOC aerogels are stable at 250 °C and start to oxidize in air only above 350 °C (Bruzzoniti et al. 2018).

 After thermal treatment, the regenerated material was characterized by FT-IR and XPS spectroscopies (see Supplementary Data) and tested for adsorption process in order to investigate its reusability.

Real sample analysis

A synthetic textile wastewater prepared as Spagni (Spagni et al. 2010), as well as a river water sample (Po river, Turin, Italy) were tested in order to assess the removal of MB from these matrices. Details on sample compositions and adsorption tests are given in the Supplementary Data section.

Results and discussion

SiC and SiOC aerogels show specific surface area of 102 and 163 m^2/g as well a total pore volume of 0.394 and 0.723 cm^3/g respectively. SiC aerogel shows mesopores in the range 20-90 nm with a maximum around 50 nm. SiOC aerogel contains mesopores in the 10-80 nm range with a maximum around 30 nm. Finally, considering that both aerogels have also larger meso/macro pores up to 200-300 nm, which are the result of the aerogel process and are not detected by the physisorption analysis, we can conclude that these samples truly demonstrate hierarchical porosity (Bruzzoniti et al. 2018).

SiC foam is a reticulated, X-ray amorphous, open cell foam with cell, window and strut sizes of 490, 170 and 55 µm respectively, 93% open porosity and SSA lower than 1 m^2/g (Bruzzoniti et al. 2018).

The adsorption studies for MB and RB were carried out at pH 5; this value is compatible with other treatment processes in the WWTPs, like coagulation processes. At pH 5 (Fig. 1S of Supplementary Data section), MB has a positive sulfur atom in the condensed rings, while RB, a xanthene dye which contains auxochrome $=NR_2^+$, is both present in the zwitterionic (82%) and positively charged (15%) form (ChemAxon Ltd. 2016).

Adsorption kinetics

Adsorption is an heterogeneous process that involves physical, chemical and electrostatic interactions (Meng et al. 2015), mainly affected by contact time between adsorbent and adsorbate. The adsorption kinetics were studied for the synthesized aerogels and foam. In parallel, a possible reduction of MB to the *leuco* form (colorless, λ_{max}=256 nm) was also monitored throughout all

adsorption experiments. For this purpose, the absorbance of each solution put in contact with the sorbents was measured at 256 nm. Since the leuco-MB was not observed, all adsorption data must be ascribed to the adsorption of MB onto the sorbents. Adsorption data for 1 mg/L MB and RB are shown in Fig. 1 and 2, respectively.
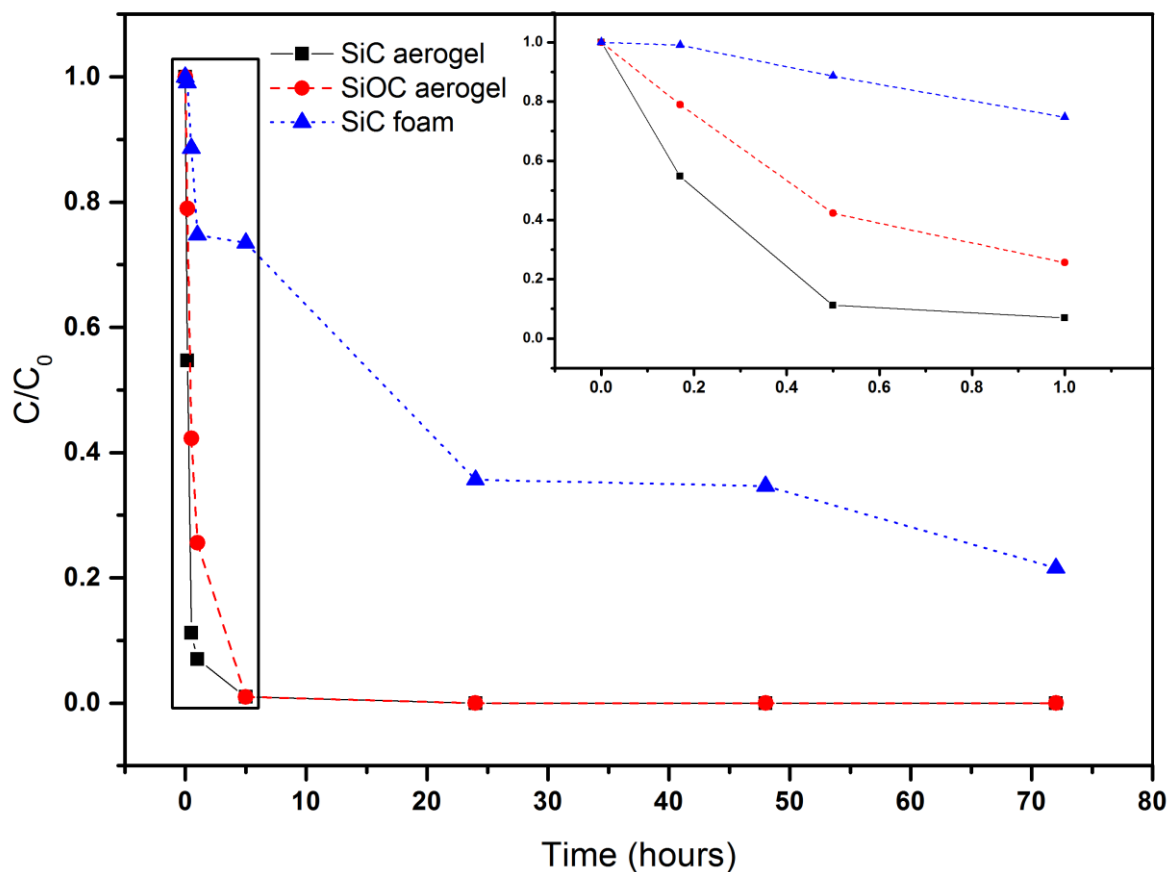

Figure 1. Adsorption kinetics for MB (C_0=initial concentration=1 mg/L, 17.5 mL, pH 5) on 0.1 g SiC foam/SiC aerogel/SiOC aerogel. C=concentration in the solution after time t.
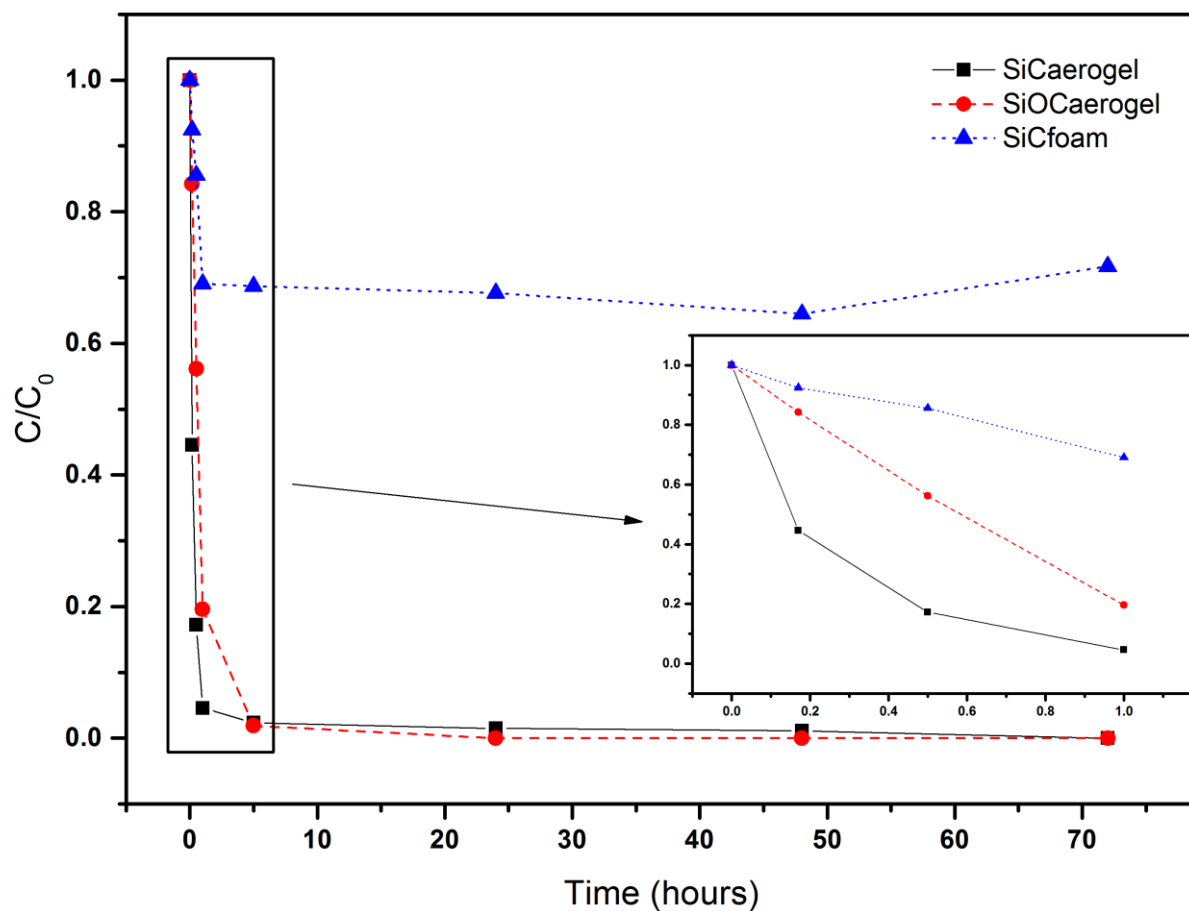
Figure 2. Adsorption kinetics for RB (C_0=initial concentration=1 mg/L, 17.5 ml, pH 5) on 0.1 g SiC foam/ SiC aerogel/ SiOC aerogel. C=concentration in the solution after time *t*.

For all the tested materials, dyes removal increases with contact time. Better performances were observed for aerogels than SiC foams.

Data obtained show that adsorption of dyes on both aerogels (SiC and SiOC) is very rapid, since more than 85% of the total adsorption takes place within the first hour of contact, and quantitative removal is achieved within 5 hours. On the contrary, the removal behaviour of SiC foam is dependent upon the dye and is not higher than 70% MB and 30% for RB.

The higher adsorption percentages observed for aerogels in respect to the foams are ascribed to the specific surface area of aerogels (163 m^2/g for SiOC and 102 m^2/g for SiC (Bruzzoniti et al.

2018)), about 100 times higher than that of SiC foam (<1 m^2/g). It is worth noting that despite the negligible SSA, the SiC foam shows a relevant capacity of adsorption towards both MB and RB.

The removal of MB and RB by the aerogels is quantitative. The meso-pores of SiOC aerogel are in the range 10 – 80 nm with a maximum around 30 nm, therefore they are fully compatible with the dimensions of the two dyes (molecular radius MB= 0.835 nm; molecular radius RB= 0.919 nm); so, no steric hindrance effects differentiate the accessibility of SiOC pores. Adsorption may be ascribed to the presence of sp^2 free carbon phase, which is a common feature of polymer derived ceramics of the Si-C-O system. For the SiC and SiOC aerogels the amount of free carbon has been estimated by measuring the weight loss of the samples when heated in air up to 1000 °C. Accordingly, 61.5 and 42.4 wt% of free carbon has been estimated for the SiC and SiOC aerogels respectively (Bruzzoniti et al. 2018). Van der Waals interactions between the graphitic phase and the aromatic structure of the dyes are proposed (Meng et al. 2015) as mechanism governing the dye adsorption.

SiC foams are characterized by lower amount of graphitic phase than the aerogels and by oxygenated surface groups, such as silanols and siloxanes groups, as revealed by FTIR (Jana et al. 2016). Owing to the above-mentioned surface characteristics, a different adsorption mechanism is expected for the SiC foam. In details, at pH 5, dissociated silanols groups interact with positively charged dyes. The lower adsorption observed for RB (28.3% after 72h), in respect to MB (78% after 72 hours), should be ascribed to the fact that only 15% RB is present as cation.

Focusing on the performances of the two aerogels materials, it should be highlighted that just after 30 minutes of contact, SiC aerogel appears to break up finely in the solution, and after 5 hours is completely dispersed, differently from SiOC aerogel that maintained its monolithic structure during the whole experiment. The stability of the sorbent is an important characteristic since it allows for an easy separation of the sorbent from the solution after the treatment. The different stability of the two aerogels may account for the different kinetics observed during the first hour of adsorption (see inset of Figure 2), in that the fragmentation of SiC aerogel may favour diffusion and adsorption.

Further experiments were aimed to test removal performance at high MB concentration (100 mg/L), which better simulates the content of MB in textile wastewaters (Ghaly et al. 2014). For its good adsorption properties and because it remains monolithic during the whole adsorption test, SiOC was selected for this investigation. The effect of initial dye concentration on color removal rate is reported in Fig. 2S (Supplementary Data), where it is shown that a removal percentage of 95.3% was achieved after 72 h. It was observed that the kinetics is slower for higher concentrations of MB. This behaviour was interpreted with the formation of MB aggregates (Patil et al. 2000) that slow down the diffusion process.

The adsorption data of MB and RB obtained for the SiOC aerogel were fitted to pseudo-first-order and pseudo-second-order kinetics models (Table 1).

Table 1. Pseudo-first-order and pseudo-second-order kinetic parameters for MB and RB adsorption on SiOC aerogel.

Analyte	Conc. (mg/L)	$q_{e(exp)}$ (mg/g)	Pseudo-first-order			Pseudo-second-order		
			$q_{e(the)}$ (mg/g)	R^2	k_1 (1/min)	$q_{e(the)}$ (mg/g)	R^2	h (mg/(g·min))
RB	1.00	0.164	0.128	0.9539	$2.95 \cdot 10^{-2}$	0.166	0.9999	0.00622
MB	1.00	0.167	0.134	0.9886	$3.41 \cdot 10^{-2}$	0.168	0.9999	0.00839
MB	100	15.7	9.64	0.9138	$1.07 \cdot 10^{-3}$	16.0	0.9951	0.0610

Briefly, the pseudo-first-order model (Lagergren's equation) describes adsorption in solid-liquid system based on the sorption capacity of solid(Randhawa et al. 2013). In its linearized form, it can be expressed by Eq.2:

$$\ln(q_e - q_t) = lnq_e - \frac{k_1}{2.303}t \qquad (2)$$

where q_e and q_t (mg/g) are the amounts of dyes adsorbed on adsorbent at equilibrium and at time t respectively and k_1 (1/min) is the rate constant of pseudo-first-order adsorption. To fit the data,

q_e was assigned at the experimental value observed at 1440 min for 1 mg/L RB and 1 mg/L MB and at 10320 min for 100 mg/L MB, since these contact times represent equilibrium conditions. The slope and intercept values of plot $ln(q_e-q_t)$ vs t were used to determine pseudo-first-order rate constant (k_1) and theoretical amount of dye adsorbed per unit mass of adsorbent ($q_{e(the)}$), respectively.

The pseudo-second-order model can be represented, in its linearized form, by Eq. 3 (Dursun and Kalayci 2005):

$$\frac{t}{q_1} = \frac{1}{k_2 q_e^2} + \frac{t}{q_e} \quad (3)$$

where k_2 (g/(mg •min)) is the pseudo-second-order rate constant of adsorption and $k_2 q_e^2$ (mg/(g•min)) is the initial adsorption rate (Randhawa et al. 2013). The values of q_e and k_2 were determined from the slope and intercept of the plots of t/q_t against t, and then the constant k_2 is used to calculate the initial sorption rate h (mg/(g•min)) at t→0. As shown in Table 1, the pseudo-second-order model provided higher correlation coefficients than the pseudo-first order model. In addition, differently from the pseudo-first-order model, the pseudo-second order model provided theoretical q_e values in agreement with the experimental q_e values for RB and for MB at the two concentration levels studied. Consequently, in accordance with the pseudo-second order reaction mechanism, chemisorption mechanism predominates in adsorption process (Kumar et al. 2005; Vadivelan and Kumar 2005). This behavior is in agreement with the presence of graphitic carbon in the surface of SiOC. In facts, pseudo-second-order adsorption kinetics have been observed for carbon nanotubes (Yao et al. 2010) and perlite (Doğan et al. 2004) for MB removal and active carbon derived from agricultural by-product for RB (Gad and El-Sayed 2009).

It is widely assumed that adsorption of compounds from solution by porous adsorbents proceeds in three consecutive steps, namely: transport of the solute molecules from the aqueous phase to the surface of the solid (film or external diffusion); transfer of solutes from the surface to the intra-

particle sites (intra-particle diffusion); adsorption of solutes on the interior surfaces of the adsorbent (Weber 1964).

Based on the Weber-Morris model, when the intra-particle diffusion is the rate-controlling step, the uptake varies almost proportionately with the half-power of time ($t^{0.5}$) and it can be expressed as (Fierro et al. 2008):

$$q_t = k_{id}\, t^{0.5} + \theta \tag{4}$$

where k_{id} is the intra-particle diffusion rate constant (mg/(g•min$^{0.5}$)), q_t (mg/g) is the amount of dyes adsorbed at time t. The value of θ (mg/g) is a constant related to the thickness of the boundary layer.

The values of k_{id} and θ are obtained by fitting q_t vs $t^{0.5}$. When intra-particle diffusion is the sole rate-limiting step, the plot of q_t versus $t^{0.5}$ yields a straight line passing through the origin(Olu-Owolabi et al. 2014).

The amount of sorbed RB and MB (q_t) for initial concentration of 1 mg/L are plotted *vs* t $^{0.5}$ in Fig. 3a. A straight line passing through the origin is observed, revealing that intra-particle diffusion is the adsorption rate controlling step. The calculated intra-particle diffusion parameters are summarized in Table 2.
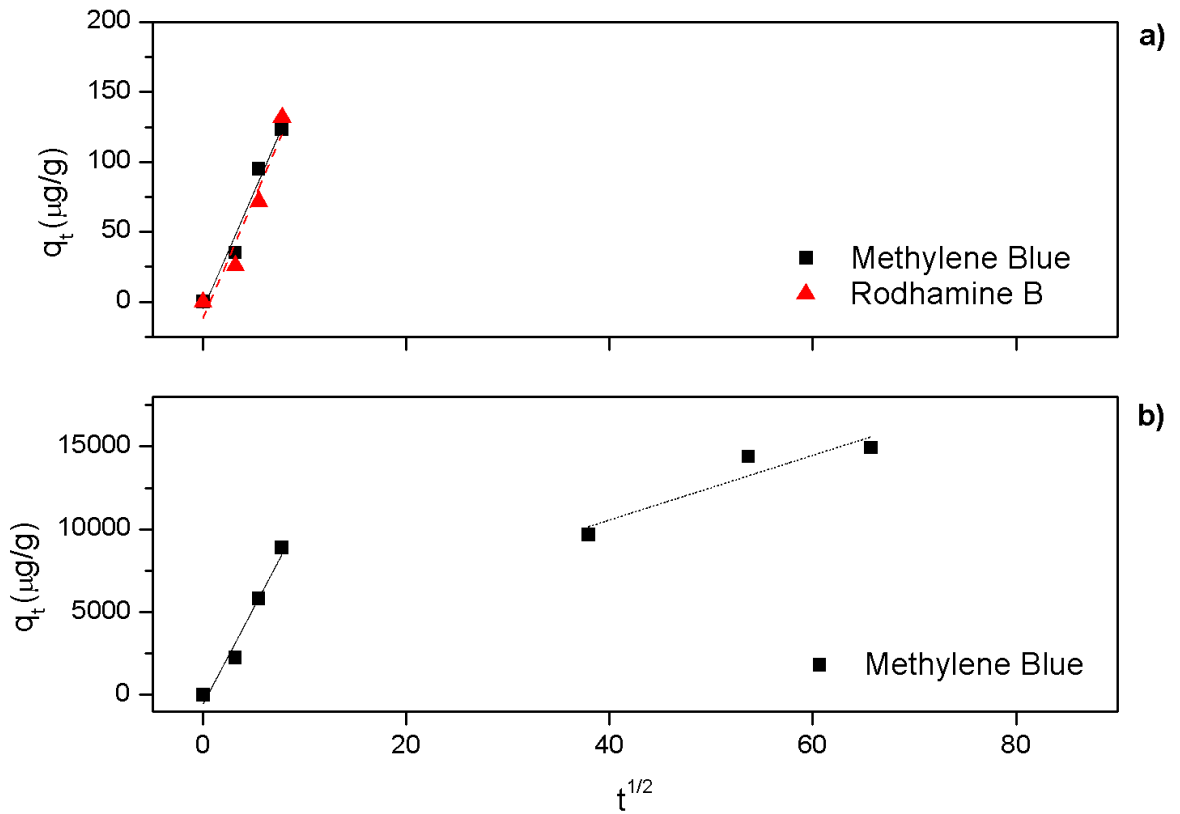
Figure 3. Intra-particle diffusion model for dyes adsorption onto SiOC aerogel: (a) 1 mg/L MB and RB, (b) 100 mg/L MB.

Table 2. Intra-particle diffusion parameters.

Dye	Conc. (mg/L)	K_{1d} (mg/(g•min$^{0.5}$))	R^2	K_{2d} (mg/(g•min$^{0.5}$))	θ (mg/g)	R^2
RB	1	0.0169	0.9375			
MB	1	0.0167	0.9721			
MB	100	1.163	0.9733	0.195	2.76	0.8787

For 100 mg/L MB, a multi-linear plot is instead observed (Fig. 3b). It is usually assumed that when data exhibit multi-linear plot, then two or more steps influence the sorption process (Fierro et al. 2008). Considering the occurrence of MB aggregation at this concentration (Tafulo et al. 2009), we propose that in this case the initial linear trend represents the film diffusion, whereas the second

less steep portion of the curve represents the sorption when intra-particle diffusion within the pores is rate-limiting (Olu-Owolabi et al. 2014).

Indeed, the slope of the initial linear portion for the two concentrations is dramatically different (two orders of magnitude) strongly suggesting that the mechanism controlling the adsorption in the two cases is not the same.

Adsorption isotherm for SiOC aerogel

Adsorption isotherm provides fundamental physicochemical data for evaluating the applicability of adsorption process (Kumar et al. 2005). Due to its promising stability and performance, adsorption isotherm was determined for the SiOC aerogel (Fig. 4). Experimental data obtained were fitted to three common isotherm models: Langmuir, Freundlich and Temkin models. Details of the used models can be found elsewhere (Bruzzoniti et al. 2016; Bruzzoniti et al. 2012).
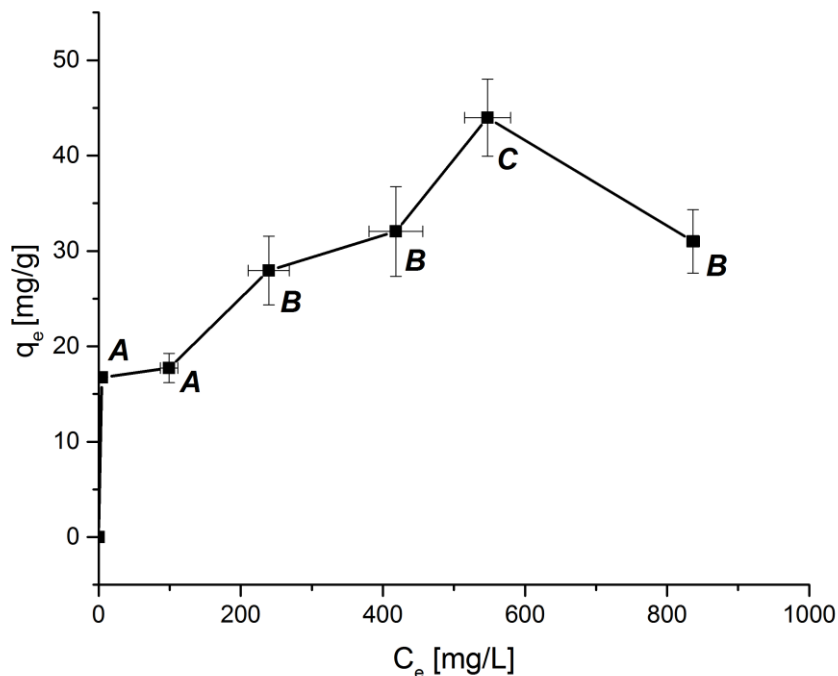

Figure 4. MB adsorption isotherm on SiOC aerogel. Experimental conditions: 0.1 g SiOC aerogel in contact with 17.5 mL of MB solutions (pH 5, range 100-1000 mg/L), stirred at room

temperature for 172 hours. Values of q_e with a letter in common are not statistically different according to the Tukey test at the 5% probability level.

The first vertical portion of the curve is ascribed to an irreversible adsorption, in which MB, below 100 mg/L, is almost completely adsorbed (removal percentage= 95.3%, q_e= 16.7 mg/g). The remaining part of the curve may be attributed to a H4 Langmuir and it is characterized by one plateau and one maximum at C_e 547 mg/L. Curves with additional rise and plateau are usually representative of multilayer adsorption and they are associated with the involvement of two different adsorption layers. The second new surface involved in the adsorption could be described by two models. In detail, the fresh surface may be: (i) the exposed parts of the layer already present (i.e. MB adsorbed); (ii) a portion of the original surface which may become uncovered by re-orientation of the MB molecules already adsorbed (e.g. from a flat to a vertical position). After the plateau, a maximum is observed instead of the second plateau typical of the H4 Langmuir. The decreasing uptake which gives rise to the maximum is tentatively ascribed to solute-solute attraction which at increasing concentration may favor MB self-aggregation, prevailing over substrate-solute attraction.

Concerning the fundamental physicochemical data, the adsorption capacity (Q_0) is a parameter usually determined to characterize the adsorbent and to compare its performance with those of other substrates (Fierro et al. 2008). Since our experimental data do not fit a L2 Langmuir type model, it is not possible to obtain a straightforward calculation of Q_0 applying the Langmuir equation. However, (Fig. 4) it is possible to calculate the maximum reversibly adsorbed amount (thus not considering the irreversible contribution) for concentrations in which the self-aggregation phenomena do not prevail (below C_0=800 mg/Lcorresponding to C_e=547 mg/L). This value ranges from 16.1 to 27.5 mg/g, depending on the initial MB concentration. This value is comparable or even higher than the adsorption capacity reported for MB adsorption on different sorbents (Banerjee and Dastidar 2005; Bhattacharyya and Sharma 2005; Bulut and Aydın 2006; Tsai et al. 2006), including activated carbon (Naeem et al. 2017; Yener et al. 2008).

Regeneration and reuse of SiOC aerogel

Several regeneration procedures using different solvents (HCl, acetonitrile and isopropanol) were tested, observing that poor recovery is obtained, with highest recovery results (22%) achieved with isopropanol. On the contrary, the thermal regeneration at 250 °C for 2 h allows for a complete removal of pollutant, as demonstrated by the FTIR study. The FT-IR spectra recorded on the SiOC aerogel before, after MB adsorption and after regeneration are shown in Figure 5. In the same figure is also shown for comparison purposes the FT-IR spectrum of the SiOC aerogel, which was exposed to the same thermal regeneration treatment without being used for MB adsorption.
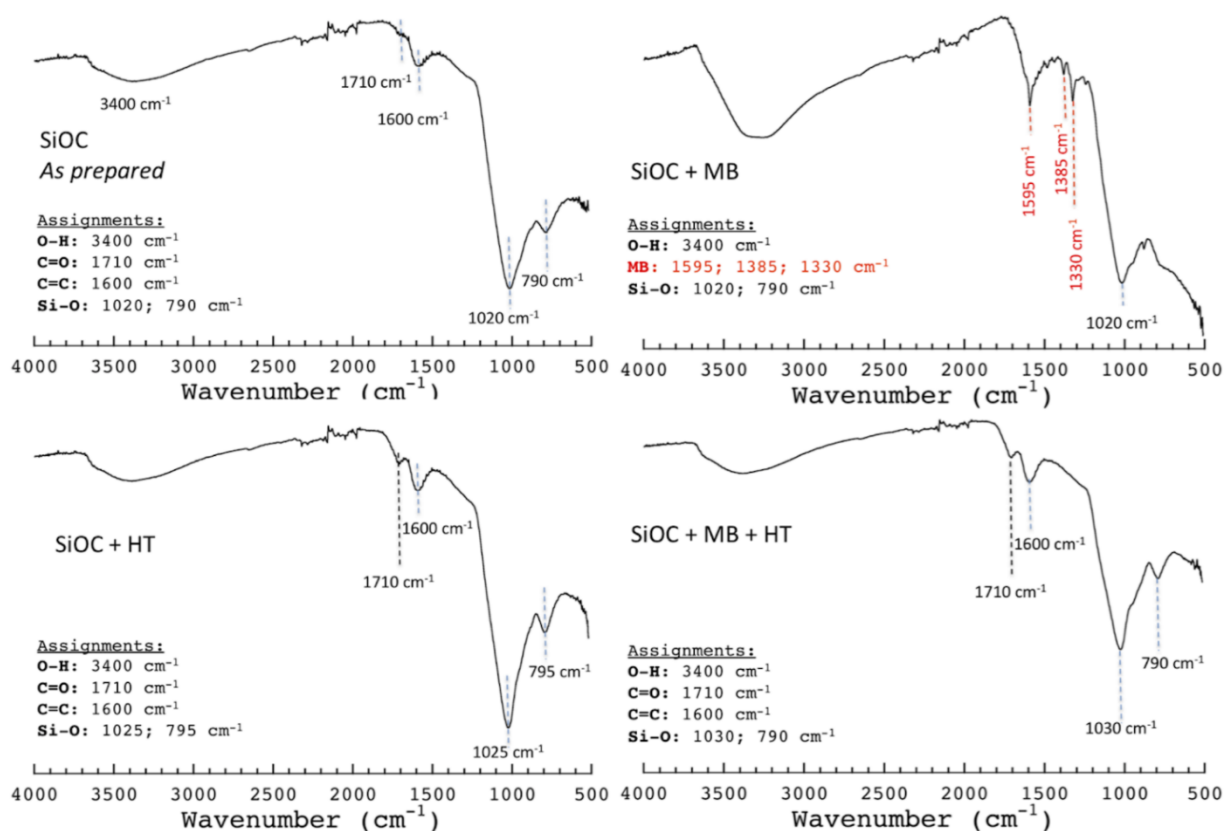

Figure 5. FT-IR spectra recorded on the SiOC aerogel samples used for the regeneration study. For details on labels, see text.

The spectrum of the "*as prepared*" sample shows peaks at 1025 and 795 cm^{-1} assigned to Si-O bonds and around 3400 cm^{-1} due to the presence of surface OH groups. The peak at 1600 cm^{-1} is assigned to C=C bonds of the free carbon phase of the silicon oxycarbide. The small shoulder at 1710

17

cm^{-1} suggests the presence of C=O bonds. The spectrum of the SiOC aerogel, which was in contact with the MB solution (SiOC + MB), clearly shows the occurrence of the adsorbed dye: new sharp peaks assigned to MB are visible at 1595, 1385 and 1330 cm^{-1} (Ovchinnikov et al. 2016). In the same spectrum, the broad peak due to OH moieties at 3400 cm^{-1} becomes more important compared to the *as prepared* sample. After thermal regeneration at 250 °C for 2 h (Sample: SiOC + MB + HT) the FT-IR spectrum does not show any more the peaks associated with the MB dye and the pattern of the starting SiOC is restored almost completely with vibrations at 1030 and 790 cm^{-1} of the Si-O bonds and at 1600 cm^{-1} of the C=C bonds of the graphitic phase. The only difference compared to the starting material is the growth of the peak at 1710 cm^{-1} which is assigned to C=O bonds belonging to carbonyl or COOH groups. The C=O functional groups (carbonyl or COOH) are most probably formed by an incipient oxidation of both graphitic phase and Si-CH$_x$, (x= 1, 2) bonds during the thermal regeneration step. Indeed, a similar FT-IR spectrum is also observed on the SiOC aerogel, which was annealed in air in the same conditions without being previously exposed to the MB solution (sample: SiOC + HT).

In order to get insights into to chemical modification occurring to the SiOC aerogels during the regeneration process, the main core levels of the elements present on the surface (O 1s, N 1s, C 1s and Si 2p) were collected on the four samples used for the regenerations studies, allowing to calculate the chemical compositions as reported in Table 1S (supplementary Data). The sample treated at 250 °C for 2 h (SiOC + HT) shows a slight increase of the oxygen content and a corresponding decrease of the C content suggesting an oxidation of the carbon present in the SiOC aerogel. This result is in agreement with the previously shown FT-IR spectra which indicate the formation of C=O moieties in the heat-treated sample. The sample which was in contact with the dye solution (SiOC + MB), shows the presence of N and an increase of the carbon amount. Both occurrences confirm the adsorption of MB on the aerogel surface. After regeneration, the samples which contained the MB (SiOC + MB + HT) shows a composition very close to the SiOC + HT sample suggesting the complete elimination of the adsorbed dye. The only difference between these

18

two aerogels (SiOC + MB + HT and SiOC + HT) is the presence of a small amount of residual N that is, most probably, directly bound to the SiOC inorganic network. The presence of N on the aerogel surface after regeneration suggests that MB is removed, at least partially, not by desorption but through a degradation process with formation of reactive N-containing fragments which bind to the aerogel surface.

The nature of the chemical bonds present on the aerogel surface was studied observing the line shape of the core level spectra. While the spectra of the Si, O and N did not give any additional information the C 1s spectrum revealed the presence of different components assigned to diverse types of chemical bonds. The C 1s spectrum of the SiOC + HT sample and its fitting components is shown, as an example, in Figure 3S. Similar fittings were performed for all the samples but the SiOC + MB. The main component at 248.6 eV can be assigned to graphitic or aliphatic CH_x, (x =1, 2) carbon atoms mainly present in the free carbon phase, the components at ~286, ~288 and at ~289 eV can be assigned to C-O, C=O and COOH bonds respectively. A similar deconvolution has also been performed for the "as prepared" SiOC aerogels and the quantitative results are reported in Table 2S. From the results reported in Table 2S we can observe that the heat treatment at 250 °C for 2 h leads to an increase of the oxygenated species and a relative decrease of the graphitic phase in agreement with the FT-IR results.

The regenerated SiOC aerogel was tested again for a new adsorption process (1000 mg/L MB, 172 h). The regenerated aerogel exhibited higher adsorption performance (recovery 42±1%) compared to those obtained for the same MB concentration, before regeneration (recovery 16±3%). The best performance obtained using the regenerated sample could be ascribed to the formation, on the aerogel surface, of new oxygenated carbon species, such as those which act as additional interaction sites with MB.

Removal of dyes from textile wastewater and from Po river water

SiOC aerogel was tested for the removal of MB from simulated textile wastewater and from a river water (Po river, Turin, Italy) sample. The rationale of these choices was to test the performance of the sorbent also in complex matrices where interfering species, namely metals at tens of ppm, organic compounds, humic and fluvic acids, could affect the removal performances via ionic and/or hydrogen-bond interactions.

The simulated textile wastewater sample was characterized by high metal content (2-50 ppm), high organic carbon load (800 mg/L chemical oxygen demand, COD), turbidity and color (see Supplementary Material).

The two samples were spiked with 1 mg/L (the concentration of visual pollution) and 150 mg/L (dye concentration used in textile processes (Ghaly et al. 2014). After 96 hours of contact, SiOC aerogel exhibits very satisfactory removal percentages for both matrices. In detail, removal of 1 mg/L MB is quantitative both from the simulated textile wastewater and from the river water samples; removal of 150 mg/L MB is 91.8% and 93.4% from the simulated textile wastewater and from the river water samples, respectively. These results indicate minimum competitive effects by the constituents of the matrix in the interaction between MB and SiOC aerogel.

Conclusions

The sorption capabilities of two types of Si-C and Si-O-C polymer derived ceramics (aerogels and foams) towards methylene blue and rhodamine B were deeply investigated. The two dyes are water soluble molecules, widely used in textile industries and hence easily found at high concentration in wastewaters to be treated in textile districts. Ceramics exhibit adsorption capabilities related not only to their SSA, but also to their surface chemistry. Unexpectedly, the SiOC and SiC PDCs showed different stability during the sorption tests; and only the SiOC aerogel remains monolithic during the entire sorption process while the SiC aerogel rapidly breaks up into fine powders. Despite the negligible SSA, the SiC foam shows a relevant capacity of adsorption towards both MB and RB. Moreover, both SiC foam and SiOC aerogels have the great advantage over other powder adsorbents

since they can be easily separated from the regenerated solution without requiring any additional filtration step. After the adsorption process, complete regeneration of SiOC is possible under moderately high temperatures for relatively short time, without atmosphere control. This regeneration step does not reduce performance of the following adsorption cycle, which indeed is further improved for the formation of oxygenated carbon species. In this regard, it should be remarked that, differently from the SiOC aerogel, activated carbon (AC), the most common adsorbent, requires regeneration at inert conditions at higher temperatures which usually reduces AC adsorption performance, due to the polymerization of residual organic compounds adsorbed and hence not completely removed. The removal capabilities of SiOC sorbent are not affected by matrix interference when tens of ppm of metal ions and several hundreds of ppm of COD are present, thus strengthening the excellent sorbent capabilities even in the presence of harsh matrices.

References

Al-Degs Y, Khraisheh M, Allen S, Ahmad M (2001) Sorption behavior of cationic and anionic dyes from aqueous solution on different types of activated carbons Sep Sci Technol 36:91-102

Baldev E, MubarakAli D, Ilavarasi A, Pandiaraj D, Ishack KSS, Thajuddin N (2013) Degradation of synthetic dye, Rhodamine B to environmentally non-toxic products using microalgae Colloids and Surfaces B: Biointerfaces 105:207-214

Banerjee S, Dastidar MG (2005) Use of jute processing wastes for treatment of wastewater contaminated with dye and other organics Bioresource Technol 96:1919-1928

Bhattacharyya KG, Sharma A (2005) Kinetics and thermodynamics of Methylene Blue adsorption on Neem (Azadirachta indica) leaf powder Dyes and Pigments 65:51-59

Bruzzoniti MC, De Carlo R, Rivoira L, Del Bubba M, Pavani M, Riatti M, Onida B (2016) Adsorption of bentazone herbicide onto mesoporous silica: application to environmental water purification Environ Sci Pollut R 23:5399-5409

Bruzzoniti MC, Appendini M, Rivoira L, Onida B, Del Bubba M, Jana P, Sorarù GD (2018) Polymer-derived ceramic aerogels as sorbent materials for the removal of organic dyes from aqueous solutions J Am Ceram Soc 101:821-830

Bruzzoniti MC, De Carlo RM, Fiorilli S, Onida B, Sarzanini C (2009) Functionalized SBA-15 mesoporous silica in ion chromatography of alkali, alkaline earths, ammonium and transition metal ions J Chromatogr A 1216:5540-5547

Bruzzoniti MC, De Carlo RM, Sarzanini C, Caldarola D, Onida B (2012) Novel insights in Al-MCM-41 precursor as adsorbent for regulated haloacetic acids and nitrate from water Environ Sci Pollut R 19:4176-4183

Bulut Y, Aydın H (2006) A kinetics and thermodynamics study of methylene blue adsorption on wheat shells Desalination 194:259-267

Caldarola D, Mitev DP, Marlin L, Nesterenko EP, Paull B, Onida B, Bruzzoniti MC, De Carlo RM, Sarzanini C, Nesterenko PN (2014) Functionalisation of mesoporous silica gel with 2-[(phosphonomethyl)-amino] acetic acid functional groups. Characterisation and application Applied Surface Science 288:373-380

ChemAxon Ltd. (2016) Chemicalize, www.chemicalize.org

Colombo P (2010) Polymer Derived Ceramics: From Nano-structure to Applications. DEStech Publications

Colombo P, Mera G, Riedel R, Sorarù GD (2010) Polymer-derived ceramics: 40 Years of research and innovation in advanced ceramics J Am Ceram Soc 93:1805-1837

Doğan M, Alkan M, Türkyilmaz A, Özdemir Y (2004) Kinetics and mechanism of removal of methylene blue by adsorption onto perlite J Hazard Mater 109:141-148

Dursun AY, Kalayci CS (2005) Equilibrium, kinetic and thermodynamic studies on the adsorption of phenol onto chitin J Hazard Mater 123:151-157

El-Ashtoukhy E-S, Fouad Y (2015) Liquid–liquid extraction of methylene blue dye from aqueous solutions using sodium dodecylbenzenesulfonate as an extractant Alexandria Eng J 54:77-81

Fierro V, Torné-Fernández V, Montané D, Celzard A (2008) Adsorption of phenol onto activated carbons having different textural and surface properties Micropor Mesopor Mater 111:276-284

Fiorilli S, Rivoira L, Calì G, Appendini M, Bruzzoniti MC, Coïsson M, Onida B (2017) Iron oxide inside SBA-15 modified with amino groups as reusable adsorbent for highly efficient removal of glyphosate from water Appl Surf Sci 411:457-465

Gad HM, El-Sayed AA (2009) Activated carbon from agricultural by-products for the removal of Rhodamine-B from aqueous solution J Hazard Mater 168:1070-1081

Ghaly A, Ananthashankar R, Alhattab M, Ramakrishnan V (2014) Production, characterization and treatment of textile effluents: a critical review J Chem Eng Process Technol 2014

Goyal R, Sreekrishnan T, Khare M, Yadav S, Chaturvedi M (2010) Experimental Study on Color Removal From Textile Industry Wastewater Using The Rotating Biological Contactor Pract Period Hazard Toxic Radioact Waste Manag 14:240-245

Gupta V (2009) Application of low-cost adsorbents for dye removal–A review J Environ Manage 90:2313-2342

Hai FI, Yamamoto K, Fukushi K (2007) Hybrid treatment systems for dye wastewater Crit Rev Env Sci Technol 37:315-377

Jana P, Bruzzoniti MC, Appendini M, Rivoira L, Del Bubba M, Rossini D, Ciofi L, Sorarù GD (2016) Processing of polymer-derived silicon carbide foams and their adsorption capacity for non-steroidal anti-inflammatory drugs Ceram Int 42:18937-18943

Jana P, Zera E, Sorarù GD (2017) Processing of preceramic polymer to low density silicon carbide foam Mater Des 116:278-286

Kumar KV, Ramamurthi V, Sivanesan S (2005) Modeling the mechanism involved during the sorption of methylene blue onto fly ash J Colloid Interface Sci 284:14-21

Melis M (2014) Additivi e tossici negli alimenti. libreriauniversitaria. it Edizioni

Meng L, Zhang X, Tang Y, Su K, Kong J (2015) Hierarchically porous silicon–carbon–nitrogen hybrid materials towards highly efficient and selective adsorption of organic dyes Sci Rep 5

Naeem S, Baheti V, Wiener J, Marek J (2017) Removal of methylene blue from aqueous media using activated carbon web The J Text I 108:803-811

Nguyen VL, Laidani NB, Sorarù GD (2015a) N-doped polymer-derived Si(N)OC: The role of the N-containing precursor J Mater Res 30:770-781

Nguyen VL, Zera E, Perolo A, Campostrini R, Li W, Sorarù GD (2015b) Synthesis and characterization of polymer-derived SiCN aerogel J Eur Ceram Soc 35:3295-3302

Olu-Owolabi BI, Diagboya PN, Adebowale KO (2014) Evaluation of pyrene sorption-desorption on tropical soils J Environ Manage 137:1-9

Ovchinnikov OV, Evtukhova AV, Kondratenko TS, Smirnov MS, Khokhlov VY, Erina OV (2016) Manifestation of intermolecular interactions in FTIR spectra of methylene blue molecules Vib Spectrosc 86:181-189

Patil K, Pawar R, Talap P (2000) Self-aggregation of methylene blue in aqueous medium and aqueous solutions of Bu 4 NBr and urea Phys Chem Chem Phys 2:4313-4317

Pereira R, Pereira M, Alves M, Pereira L (2014) Carbon based materials as novel redox mediators for dye wastewater biodegradation Appl Catal B 144:713-720

Randhawa N, Das N, Jana R (2014) Adsorptive remediation of Cu (II) and Cd (II) contaminated water using manganese nodule leaching residue Desal Water Treat 52:4197-4211

Richardson M (2008) Chemical safety: international reference manual. John Wiley & Sons

Rivoira L, Appendini M, Fiorilli S, Onida B, Del Bubba M, Bruzzoniti MC (2016) Functionalized iron oxide/SBA-15 sorbent: investigation of adsorption performance towards glyphosate herbicide Environ Sci Pollut R 23:21682-21691

Singh K, Arora S (2011) Removal of synthetic textile dyes from wastewaters: a critical review on present treatment technologies Crit Rev Environ Sci Technol 41:807-878

Spagni A, Grilli S, Casu S, Mattioli D (2010) Treatment of a simulated textile wastewater containing the azo-dye reactive orange 16 in an anaerobic-biofilm anoxic–aerobic membrane bioreactor Int Biodeter Biodegradation 64:676-681

Tafulo P, Queirós R, González-Aguilar G (2009) On the "concentration-driven" methylene blue dimerization Spectrochim Acta Mol Biomol Spectrosc 73:295-300

Tian Y, Cui G, Liu Y, Li H, Sun Z, Yan S (2016) Self-assembly synthesis of hollow double silica@ mesoporous magnesium silicate magnetic hierarchical nanotubes with excellent performance for fast removal of cationic dyes Appl Surf Sci 387:631-641

Tsai WT, Yang JM, Lai CW, Cheng YH, Lin CC, Yeh CW (2006) Characterization and adsorption properties of eggshells and eggshell membrane Bioresour Technol 97:488-493

Umoren S, Etim U, Israel A (2013) Adsorption of methylene blue from industrial effluent using poly (vinyl alcohol) J Mater Environ Sci 4:75-86

Vadivelan V, Kumar KV (2005) Equilibrium, kinetics, mechanism, and process design for the sorption of methylene blue onto rice husk Journal Colloid Interface Sci 286:90-100

Vallachira Warriam Sasikumar P, Zera E, Graczyk-Zajac M, Riedel R, Sorarù GD, Dunn B (2016) Structural Design of Polymer-Derived SiOC Ceramic Aerogels for High-Rate Li Ion Storage Applications J Am Ceram Soc 99:2977-2983

Verma AK, Dash RR, Bhunia P (2012) A review on chemical coagulation/flocculation technologies for removal of colour from textile wastewaters J Environ Manage 93:154-168

Weber WJM, J.C. (1964) Kinetics of adsorption on carbon from solution J Sanit Eng Div Am Soc Civ Eng 89:31-59

Yao Y, Xu F, Chen M, Xu Z, Zhu Z (2010) Adsorption behavior of methylene blue on carbon nanotubes Bioresour Technol 101:3040-3046

Yener J, Kopac T, Dogu G, Dogu T (2008) Dynamic analysis of sorption of methylene blue dye on granular and powdered activated carbon Chem Eng J 144:400-406

Yu Z, Feng Y, Li S, Pei Y (2016) Influence of the polymer–polymer miscibility on the formation of mesoporous SiC(O) ceramics for highly efficient adsorption of organic dyes J Eur Ceram Soc 36:3627-3635

Zera E, Campostrini R, Aravind PR, Blum Y, Sorarù GD (2014) Novel SiC/C aerogels through pyrolysis of polycarbosilane precursors Adv Eng Mater 16:814-819

SUPPLEMENTARY DATA

Regenerable, innovative porous silicon-based polymer-derived ceramics for removal of Methylene Blue and Rhodamine B from textile and environmental waters

Maria Concetta Bruzzoniti*[a], Marta Appendini[a], Barbara Onida[b], Michele Castiglioni[a], Massimo Del Bubba[c], Lia Vanzetti[d], Prasanta Jana[e], Gian Domenico Sorarù[e], Luca Rivoira[a]

[a]*Department of Chemistry, University of Turin, Via P. Giuria 7, 10125 Turin, Italy.*
[b]*Department of Applied Science and Technology, Polytechnic of Torino, Corso Duca degli Abruzzi 24, 10129 Torino, Italy.*
[c]*Department of Chemistry "Ugo Schiff", University of Florence, Via della Lastruccia 3, 50019 Sesto Fiorentino, Italy.*
[d]*Fondazione Bruno Kessler-CMM-MNF, Via Sommarive 18, 38123 Trento, Italy.*
[e]*Department of Industrial Engineering, University of Trento, Via Sommarive 9, 38123 Trento, Italy*

Determination of dyes. A Varian 9012 HPLC Gradient Pump, equipped with a 25μL loop, a reversed-phase C-18 analytical column (LiChroCart PuroSphere RP-18, 125 mm x 3.0 mm, 5 μm, Merck) was used for dyes chromatographic separation. The mobile phase was 46% of 50 mM sodium formate buffer (pH 3), and 54% CH_3CN (eluent flow rate 0.5 mL min^{-1}). Before use, eluents were filtered through 0.45 μm mixed cellulose ester membrane filters. Detection was performed by spectrophotometric detection (at 660 nm and 550 nm for Methylene blue and Rhodamine B, respectively) by a 4000i UV-Vis absorbance system (Dionex, Thermo Fisher). Limits of detection and quantification (Shrivastava and Gupta, 2011) were respectively 34 μg/L and 104 μg/L for MB,

28 µg/L and 86 µg/L[1] for RB. A Cary-60 UV-Vis spectrophotometer (Agilent Technologies) was used for the determination of the leuco-MB.
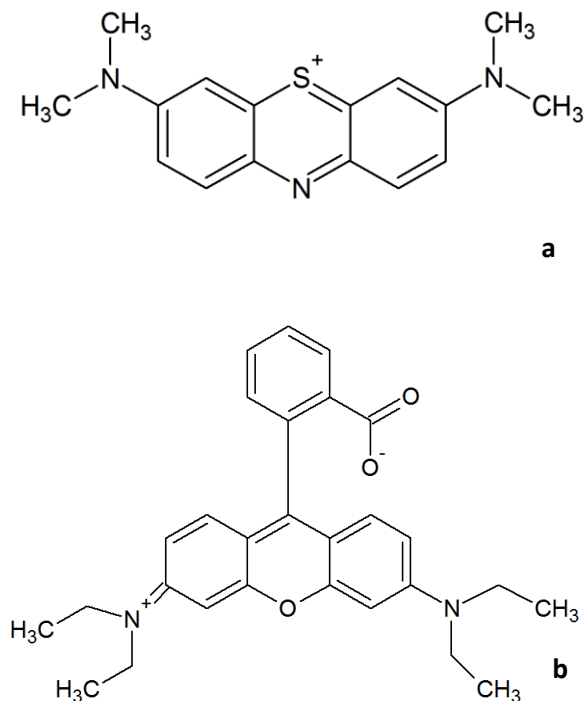

Figure 1S. Methylene blue (MB) (a) and Rhodamine B (RB) (b) structures. For RB the zwitterionic form is shown.

Adsorbent characterization. Microstructural characterization of the SiC and SiOC aerogels as well as the SiC foams was already reported in previous publications from our groups (Jana et al., 2016; Bruzzoniti et al., submitted 2017). In particular N_2 physisorption technique was used to measure the specific surface area, the total porosity and the pore size for the two ceramic aerogels (Bruzzoniti et al., submitted 2017). The SiC foam was characterized by density measurements to quantify the amount of total porosity and by SEM to get the average cell size. The specific surface area of the SiC foam was also estimated by N_2 physisorption analysis (Jana et al., 2016).

Adsorption kinetics. Tests were performed in batch conditions. Aliquots of 0.1 g of SiC foam and SiC/SiOC aerogels were put in contact with 17.5 mL of dye solutions (1 mg/L, pH 5.0)

and stirred on a rotary shaker. In order to take into account adsorption on flasks, solutions containing dyes only were processed in parallel. Samples were withdrawn at fixed time intervals (0, 10, 30, 60 min, 5, 24, 48, 72 hours), centrifuged (10000 rpm, 5 min) diluted 1:1 and analysed by HPLC.

For MB only, adsorption studies at high concentrations (100 mg/L) were also performed. Experiments were performed in triplicate, at room temperature.
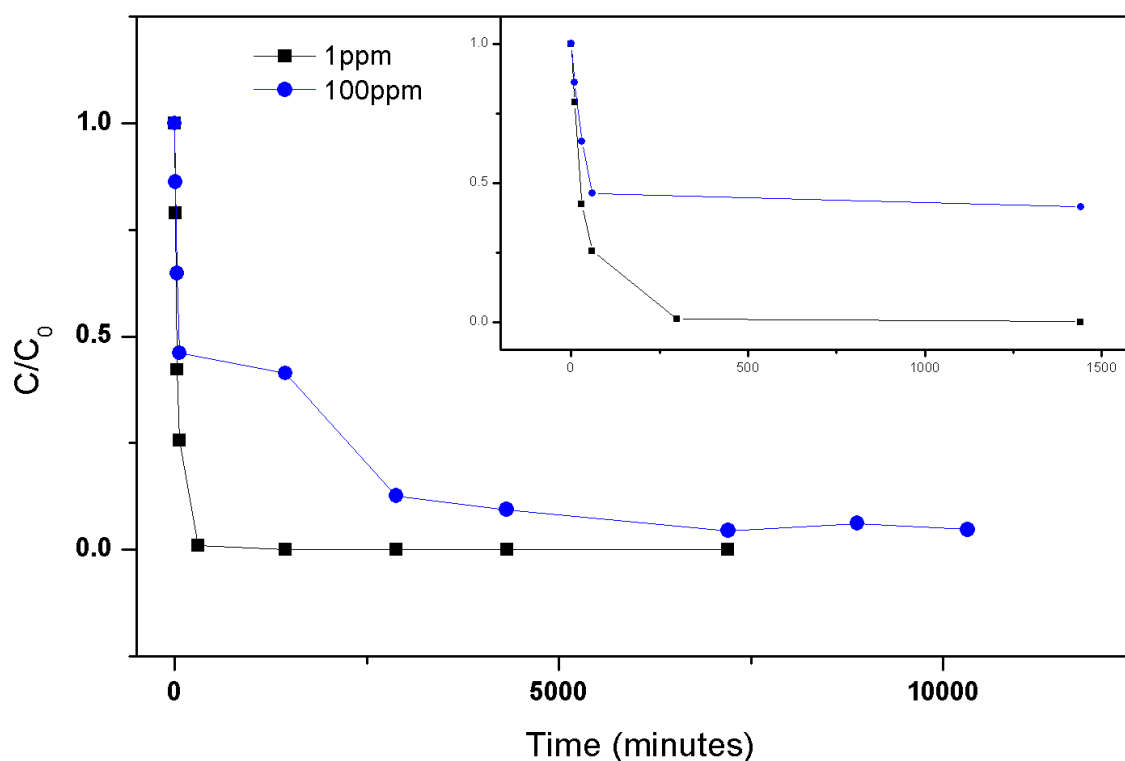

Figure 2S. Adsorption kinetics for MB (1 mgL^{-1} and 100 mgL^{-1}, at pH 5) on SiOC aerogel.

Adsorption isotherm. Equilibrium studies were performed on aliquots of 0.1 g of SiOC aerogel with 17.5 ml of MB solutions at different initial dye concentrations (pH 5), 100, 200, 400, 600, 800, 1000 mg/L. The contact was made in 50 ml-conical flasks using a rotary shaker at

constant agitation speed and room temperature, for 172 hours which is more than sufficient time to reach equilibrium, as highlighted by the kinetics studies.

A control was processed in parallel. The amount of dye adsorbed at equilibrium (q_e, mg/g) was determined as follows:

$$q_e = \frac{(C_0 - C_e)V}{m} \qquad (1)$$

where where C_0 (mg/L) and C_e (mg/L) are respectively the initial and equilibrium concentrations of dyes in solution, V (L) is the volume of solution and m (g) is the mass of the adsorbent.

The recovery percentage (R%) for each substrate was calculated by the following relation:

R% = 100 · (C_0-C_e)/C_0 (2)

Characterization of adsorbents after regeneration

After thermal treatment, the regenerated material was characterized by FT-IR and XPS spectroscopies and tested for adsorption process in order to investigate its reusability. FT-IR was performed with a Nicolet Avatar 330 Fourier transform infrared spectrometer (Thermo Electron Corporation, Waltham, MA) using KBr technique in transmission mode. An average of 64 scans with 4 cm^{-1} resolution was recorded for each specimen. XPS analyses were performed using a Kratos Axis Ultra DLD instrument (Kratos Analytical, Manchester, UK) equipped with a hemispherical analyser and a monochromatic Al Ka (1486.6 eV) X-ray source. For each sample first a survey scan (0–1200 eV, binding energy) to detect the elements present on the surface, and then the individual O 1s, N 1s, C 1s and Si 2p core lines were collected. The quantification, reported as the relative elemental percentage, was performed using the integrated area of the fitted core lines, corrected for the instrument sensitivity factors. Charge compensation, when needed, was achieved

using a charge neutralizer located at the bottom of the electrostatic input lens system and all core level peak energies were referenced to the main peak in C 1s at 284.6 eV.

Table 1S. XPS chemical composition (in atom %) of the samples used for the regeneration study.

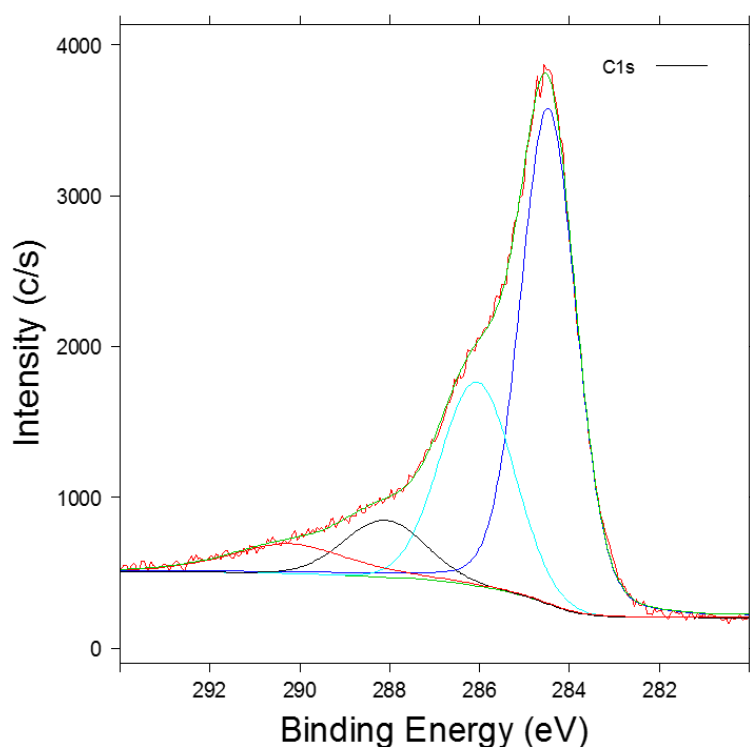| Sample	Si (at%)	C (at%)	O (at%)	N (at%)
SiOC	13.7	55.2	31.1	--
SiOC + HT	13.1	51.8	35.0	--
SiOC + MB	10.7	62.2	25.7	1.5
SiOC + MB + HT	13.7	51.3	35.4	0.7
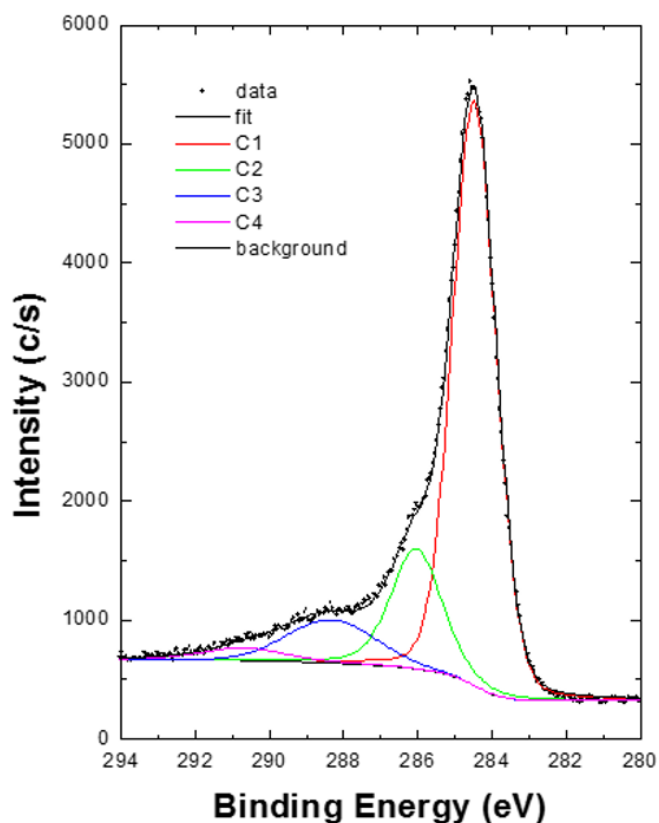
Figure 3S. C 1s spectrum recorded on the SiOC + HT sample showing the fit components.

Table 2S. Relative intensities of the C1s components (Beamson and Briggs, 1992) recorded on the "as prepared" aerogel (SiOC) and after high temperature treatment (SiOC + HT) at 250 °C for 2 h.

Sample	284.6 eV [Graphitic C]	~ 286 eV [C-O]	~ 288 eV [C=O]	~ 289 eV [COOH]	C_{Tot}
SiOC	40.8	8.8	4.1	1.5	55.2
SiOC + HT	32.0	9.2	5.1	1.5	51.8

Wastewater and river water analysis

A synthetic textile wastewater as well as a river water (Po river, Turin, Italy) sample were tested in order to assess the removal of MB from these matrices.

The simulated wastewater composition was based on the work of Spagni et al.(Spagni et al., 2010), and it composed of glucose as the main carbon source at a concentration of 800 mg/L COD, 400 mg/L NaCl, 40 mg/L NH₄Cl, 240 mg/L NaHCO₃, 56.2 mg/L K₂HPO₄, and the following salts:

20 mg/L $CaCl_2$, 50 mg/L $MgCl_2 \cdot 6H_2O$, 20 mg/L $FeCl_3$, 5 mg/L $ZnCl_2$, 5 mg/L $CoCl_2 \cdot 6H_2O$, 5 mg/L $MnCl_2 \cdot 4H_2O$, 5 mg/L $CuCl_2 \cdot 2H_2O$, 2 mg/L $Na_2MoO_4 \cdot 2H_2O$, 2 mg/L $NiCl_2 \cdot 6H_2O$, 2 mg/L $AlCl_3$, 0.5 mg/L H_3BO_3 (0.5), 0.5 mg/L Na_2SeO_3. The pH of the synthetic wastewater was 7.3.

Concerning the river water, a sample (Po river, Turin, Italy) was collected, filtered with 0.45 μm mixed cellulose ester membrane filters and stored in a Pyrex bottle at 4°C, protected from light until analysis. The pH of river water was 8.0.

Operatively, 0.1 g SiOC aerogels were put in contact with 17.5 ml of each of the real sample spiked with 1 and 150 mg/L of MB. Samples were withdrawn at different time intervals for a final collecting time of 96 hours. The samples were analyzed by HPLC to evaluate the percentage of MB adsorbed ($R_{ads}=100*(C_0-C_e)/C_0$). For the real sample analysis, the chromatographic method was adapted in order to separate the analyte peak from the matrix signal. The final conditions were: 69% of 50 mM formate buffer (pH 3) and 31% CH_3CN.

References

Beamson G, Briggs D (1992) High resolution XPS of organic polymers: the Scienta ESCA300 database. Ed. Wiley, Chichester; New York.

Bruzzoniti MC, Appendini M, Rivoira L, Onida B, Del Bubba M, Jana P, Sorarù GD (2017) Polymer-derived ceramic aerogels as sorbent materials for the removal of organic dyes from aqueous solutions J Am Ceram Soc in press doi:10.1111/jace.15241

Jana P, Bruzzoniti MC, Appendini M, Rivoira L, Del Bubba M, Rossini D, Ciofi L, Sorarù GD (2016) Processing of polymer-derived silicon carbide foams and their adsorption capacity for non-steroidal anti-inflammatory drugs. Ceram Int 42:18937-18943

Shrivastava A, Gupta VB (2011) Methods for the determination of limit of detection and limit of quantitation of the analytical methods. Chron Young Sci 2:21-25

Spagni A, Grilli S, Casu S, Mattioli D (2010) Treatment of a simulated textile wastewater containing the azo-dye reactive orange 16 in an anaerobic-biofilm anoxic–aerobic membrane bioreactor. Int Biodeterior Biodegr 64:676-681